International Journal of Antimicrobial Agents 55 (2020) 105941

Contents lists available at ScienceDirect

International Journal of Antimicrobial Agents

journal homepage: www.elsevier.com/locate/ijantimicag

Combination of polymyxin B and minocycline against multidrug-resistant *Klebsiella pneumoniae*: interaction quantified by pharmacokinetic/pharmacodynamic modelling from in vitro data

Chenyan Zhao[a], Pikkei Wistrand-Yuen[b], Pernilla Lagerbäck[b], Thomas Tängdén[b], Elisabet I. Nielsen[a], Lena E. Friberg[a,*]

[a] Department of Pharmaceutical Biosciences, Uppsala University, SE-751 24 Uppsala, Sweden
[b] Department of Medical Sciences, Section of Infectious Diseases, Uppsala University, SE-751 85 Uppsala, Sweden

ARTICLE INFO

Article history:
Received 23 September 2019
Accepted 5 March 2020

Editor: Jian Li

Keywords:
Polymyxin B
Minocycline
Combination therapy
Pharmacokinetic/pharmacodynamic model
In vitro time–kill study
Multidrug-resistant *Klebsiella pneumoniae*

ABSTRACT

Lack of effective treatment for multidrug-resistant *Klebsiella pneumoniae* (MDR-Kp) necessitates finding and optimising combination therapies of old antibiotics. The aims of this study were to quantify the combined effect of polymyxin B and minocycline by building an in silico semi-mechanistic pharmacokinetic/pharmacodynamic (PKPD) model and to predict bacterial kinetics when exposed to the drugs alone and in combination at clinically achievable unbound drug concentration–time profiles. A clinical *K. pneumoniae* strain resistant to polymyxin B [minimum inhibitory concentration (MIC) = 16 mg/L] and minocycline (MIC = 16 mg/L) was selected for extensive in vitro static time–kill experiments. The strain was exposed to concentrations of 0.0625–48 × MIC, with seven samples taken per experiment for viable counts during 0–28 h. These observations allowed the development of the PKPD model. The final PKPD model included drug-induced adaptive resistance for both drugs. Both the minocycline-induced bacterial killing and resistance onset rate constants were increased when polymyxin B was co-administered, whereas polymyxin B parameters were unaffected. Predictions at clinically used dosages from the developed PKPD model showed no or limited antibacterial effect with monotherapy, whilst combination therapy kept bacteria below the starting inoculum for >20 h at high dosages [polymyxin B 2.5 mg/kg + 1.5 mg/kg every 12 h (q12h); minocycline 400 mg + 200 mg q12h, loading + maintenance doses]. This study suggests that polymyxin B and minocycline in combination may be of clinical benefit in the treatment of infections by MDR-Kp and for isolates that are non-susceptible to either drug alone.

1. Introduction

Management of antimicrobial resistance in multidrug-resistant *Klebsiella pneumoniae* (MDR-Kp) is a major challenge for clinicians [1]. Carbapenem-resistant and extended-spectrum β-lactamase (ESBL)-producing *K. pneumoniae* are listed as one of the most critical priority pathogens by the World Health Organization (WHO) (https://www.who.int/medicines/publications/WHO-PPL-Short_Summary_25Feb-ET_NM_WHO.pdf). Infections caused by these bacteria, e.g. urinary tract infections, nosocomial pneumonia and bloodstream infections, are associated with high mortality rates in critically ill patients [2]. Polymyxin B (PMB) and polymyxin E (colistin) have been revived as last-resort treatment options for these infections. However, the alarming increase in resistance to polymyxins [3] necessitates optimising the use of these antibiotics. Polymyxin-based combination therapy has been suggested to enhance and preserve antibacterial activity [4]. In a previous screening experiment, minocycline (MIN) was identified among 13 tested old antibiotics as a promising companion drug to PMB, showing a synergistic effect [$\geq$2 $\log_{10}$ colony-forming unit (CFU)/mL reduction with the combination compared with its most active constituent at 24 h] in four of five carbapenem-resistant *K. pneumoniae* clinical isolates [5]. Among the four strains, *K. pneumoniae* ARU613 was considered as the most refractory, being non-susceptible to both drugs with minimum inhibitory concentrations (MICs) of 16 mg/L both for PMB and MIN.

* Corresponding author. Present address: Department of Pharmaceutical Biosciences, Uppsala University, P.O. Box 591, SE-751 24 Uppsala, Sweden. Tel.: +46 18 471 4685; fax: +46 18 471 4003.
E-mail address: lena.friberg@farmbio.uu.se (L.E. Friberg).

https://doi.org/10.1016/j.ijantimicag.2020.105941

In vitro time–kill studies have advantages over in vivo experiments since they are less resource demanding. Their use is recommended by the European Medicines Agency (EMA) to provide insight into exposure–effect relationships [6]. In vitro static time–kill studies are relatively easy and inexpensive compared with dynamic experiments, but with the drawback that drug concentrations are constant. However, by in silico semi-mechanistic pharmacokinetic/pharmacodynamic (PKPD) modelling, knowledge gained from static time–kill studies can be extended to dynamic systems, as shown for instance for *Streptococcus pyogenes* exposed to five antibiotics of different classes [7]. With this approach, a range of different dosing regimens and scenarios of interest can be compared before conducting clinical studies.

PKPD modelling has additional advantages in exploring effective drug combinations [8]. When studying combinations, the number of possible permutations of dosages and PK profiles of interest quickly becomes unfeasible to be tested experimentally. However, the number of tests is in principle unlimited in model simulations. In addition, PKPD models provide insight into the relative contribution of the component drugs to the overall effect.

The aim of this study was to predict the clinical effect of PMB and MIN against MDR-Kp, by first performing richly sampled in vitro static time–kill studies of both drugs alone and in combination against *K. pneumoniae* ARU613, followed by building an in silico PKPD model characterising the observations from these experiments. Predictions were thereafter conducted by linking published PK models to the developed PKPD model to perform Monte Carlo simulations. This study also serves as an example where a modelling approach is applied for translation of antibiotic effects from in vitro to a clinical setting against a strain non-susceptible to either antibiotic alone.

2. Materials and methods

The study was carried out stepwise. First, PMB and MIN monodrug time–kill studies were conducted and PKPD models were built based on their respective data set. Subsequently, the monodrug PKPD models were combined with shared bacteria-related parameters and were re-estimated to fit the combined monodrug data. Predictions assuming an additive combined effect were then made to facilitate the selection of concentrations to be tested experimentally [9]. When combination data were available, the PKPD model was updated to fit the whole (two monodrugs + their combination) data set. To note, drug adsorption to plastics [10] and degradation were considered in the modelling. The final developed PKPD model was linked to published PK models for MIN [11] and PMB [12] in order to predict the combined drug effect in a simulated patient population by letting the predicted unbound concentration drive the drug effect.

2.1. Strains, growth media and antibiotics

A clinical OXA-48-producing MDR-Kp isolate (strain ARU613) originating from a wound of a patient in Sweden was kindly provided by the Public Health Agency of Sweden. MICs were determined at least in duplicate by broth microdilution (for PMB), agar dilution (fosfomycin) or a gradient method (other antibiotics; Etest, bioMérieux, Marcy-l'Étoile, France) and the median values were as follows: amikacin, 128 mg/L; aztreonam, 128 mg/L; cefepime, 256 mg/L; ceftazidime, 8 mg/L; ciprofloxacin, >32 mg/L; chloramphenicol, >256 mg/L; ertapenem, >32 mg/L; fosfomycin, 256 mg/L; gentamicin, 128 mg/L; meropenem, 32 mg/L; MIN, 16 mg/L; PMB, 16 mg/L; tigecycline, 2 mg/L; and trimethoprim, >32 mg/L. Strain ARU613 is thus categorised as resistant to all of the abovementioned antibiotics according to Clinical and Laboratory Standards Institute (CLSI) (PMB and MIN) and European Committee on Antimicrobial Susceptibility Testing (EUCAST) (other antibiotics) clinical breakpoints [13,14]. Mueller–Hinton II broth and agar (BD Diagnostics, Sparks, MD, USA) were used as growth media. PMB sulphate salt and MIN hydrochloride were purchased from Merck KGaA (Darmstadt, Germany). Meropenem resistance was probably mainly caused by the presence of bla_{OXA-48}, and PMB resistance by a mutation in the *crrB* gene (N311T) as determined by whole-genome sequencing [5].

Table 1
Minocycline (MIN) and polymyxin B (PMB) nominal concentrations used in the combination experiments.

Experiment no.	MIN concentration (mg/L)	PMB concentration (mg/L)
1	1.5	1
2	1.5	4
3	1.5	8
4	3	1
5	3	2
6	3	4
7	6	1
8	6	4
9	12	1

Stock solutions (10 g/L) were freshly prepared by dissolving PMB in water and MIN in dimethyl sulfoxide (DMSO), and then further diluted to desired concentrations in water. All solutions were protected from light. Incremental dilutions in polypropylene tubes (Falcon™; BD Diagnostics) were performed to minimise non-specific drug adsorption [10]. When experiments with DMSO concentrations >1% [14] were omitted from the estimation (MIN concentrations of 192, 384 and 768 mg/L), similar parameter estimates and visual predictive checks (VPCs) were obtained as when those experiments were included.

2.2. Time–kill experiments

In monodrug experiments, the strain was exposed to nominal PMB concentrations of 1–128 mg/L (i.e. 0.0625–8 × MIC) or MIN concentrations of 1.5–768 mg/L (i.e. ~0.1–48 × MIC), increasing in a two-fold manner. Experiments were performed at least in duplicate. Nominal concentrations of the nine selected antibiotic pairs for the combination experiments (performed in triplicate) are listed in Table 1. Bacterial cultures were prepared to achieve a starting inoculum in exponential growth phase of ~5 × 10^6 CFU/mL. A growth control was included in every experiment, and monodrugs (1 × MIC for PMB and 0.75 × MIC for MIN) were included in all combination experiments as a reference. Tubes were incubated at 37 °C with shaking at 190 rpm during the entire experiment. Samples were collected before adding antibiotics (0 h) and after 1, 2, 4, 8, 24 and 28 h of incubation in the presence of antibiotics. Samples were serially (ten-fold) diluted before plating on agar and then viable counts, i.e. the number of CFU on the plates, were counted following overnight incubation at 37 °C [9]. The limit of detection (LOD) was 10 CFU/mL.

2.3. Measured drug concentrations

Samples from bacteria-free tubes containing 0.25–8 mg/L PMB (two-fold increase) were drawn at 0 h and 4 h (in triplicate) for drug concentration analysis. In a pilot experiment, the loss was found to be negligible after 4 h, in line with what has been reported for colistin [10]. Each sample (200 µL) was transferred to an Eppendorf tube filled with 200 µL of human serum (to prevent further binding to the new tube [15]) and was stored at –20 °C until analysis. Sample preparation was performed in the same manner as described for colistin [15] and the sample was quantified by liquid chromatography–tandem mass spectrometry

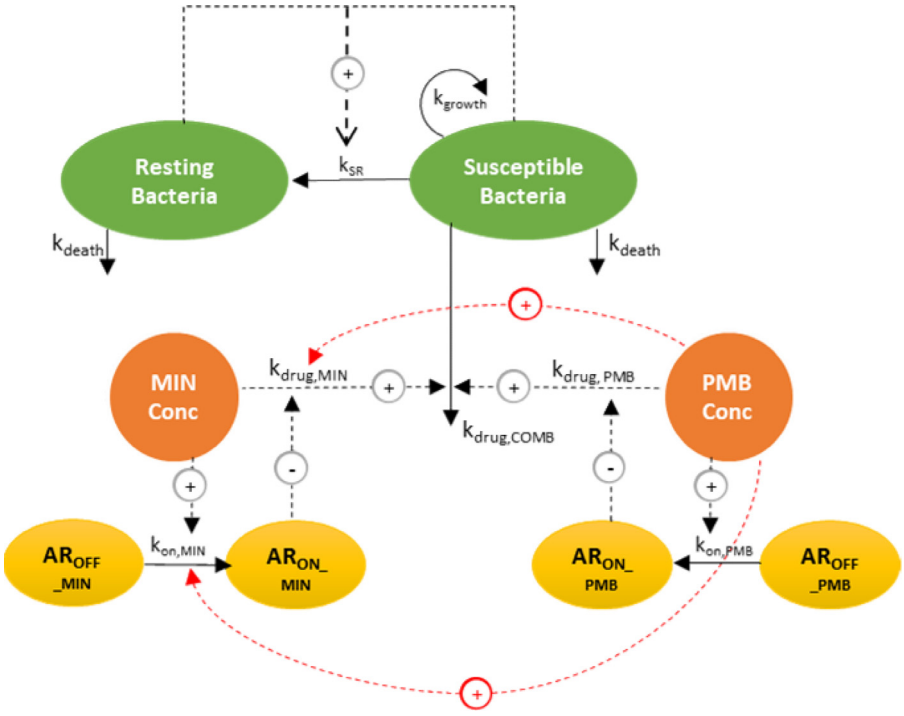

Fig. 1. Schematic illustration of the final pharmacokinetic/pharmacodynamic model for polymyxin B (PMB) and minocycline (MIN) drug combination against *Klebsiella pneumoniae*. Bacteria transfer from drug-susceptible, growing state to non-susceptible, non-growing resting state (green). Antibiotic concentrations (orange) are related to the drug-induced killing effect through rate constants ($k_{drug,MIN}$ and $k_{drug,PMB}$), and the effect is diminishing by accumulated adaptive resistance (AR_{ON_MIN} and AR_{ON_PMB}, yellow). The adaptive resistance onset rate constant ($k_{on,MIN}$ and $k_{on,PMB}$) increases with increasing drug concentrations. The combined antibacterial killing rate constant ($k_{drug,COMB}$) is dependent on $k_{drug,MIN}$ and $k_{drug,PMB}$. In combination therapy, PMB elevated $k_{drug,MIN}$ and $k_{on,MIN}$ in a concentration-dependent manner (red dashed lines).

(LC-MS/MS) on a Sciex QTRAP 6500 LC-MS/MS system (Sciex) coupled to a Waters ACQUITY UPLC (ultra performance liquid chromatography) system (Waters Corp., Milford, MA, USA). All samples were assayed on the same day. The linearity range was 0.1–10 mg/L, with intrarun variability of 1–12% in the concentration range of 0.2–10 mg/L. The PMB concentration was assumed to decrease exponentially between 0 h and 4 h according to Eq. 1:

$$\frac{dC}{dt} = -k_d \cdot C \tag{1}$$

where the means of the measured concentrations (C) at 0 h and 4 h were used to determine the first-order rate constant (k_d) for each nominal concentration. The MIN loss was set to be negligible (half-life >40 h) based on observations in a pilot experiment where nominal drug concentrations of 3, 24 and 96 mg/L were analysed and the intrarun assay variability ranged between 8–14% in the linear concentration range of 0.1–100 mg/L.

2.4. In silico pharmacokinetic/pharmacodynamic model building

2.4.1. Bacterial growth model

A self-limiting bacterial growth model was applied [16]. Bacteria started (0 h) in the drug-susceptible, growing state (S) and were transferred to the non-susceptible, non-growing resting state (R) as a response to the total bacterial load. A reversal transfer was set to 0 as it was not supported by the data. A delay in transfer from S to R [17] was tested. The schematic of the model can be found in Fig. 1 (green part) with differential equations (Eq. 2–4) illustrating their relationships.

$$\frac{dS}{dt} = k_{growth} \cdot S - \left(k_{death} + k_{drug} \cdot Inh_{AR}\right) \cdot S - k_{SR} \cdot S \tag{2}$$

$$\frac{dR}{dt} = k_{SR} \cdot S - k_{death} \cdot R \tag{3}$$

$$k_{SR} = \frac{S+R}{B_{\max}} \cdot (k_{growth} - k_{death}) \tag{4}$$

where k_{growth}, k_{death} and k_{SR} are the rate constants of bacterial growth, death and transfer from S to R, respectively; B_{max} is maximum bacterial load; and k_{drug} and Inh_{AR} are drug-related parameters and are discussed below.

2.4.2. Monodrug modelling

The drug-related part of the model consisted of the drug killing rate constant k_{drug} and the inhibition of k_{drug} owing to adaptive resistance (Inh_{AR}), as illustrated in Fig. 1. Since similar structures were tested for both monodrug models, the equations below are presented without specification for drugs, i.e. k_{drug} and Inh_{AR} represent either $k_{drug,PMB}$ and $Inh_{AR,PMB}$ or $k_{drug,MIN}$ and $Inh_{AR,MIN}$. Tested functions for k_{drug} were a sigmoid ($\gamma \neq 1$) and a basic ($\gamma = 1$) E_{max} function (Eq. 5) and a power ($\gamma \neq 1$) and a linear ($\gamma = 1$) function (Eq. 6).

$$k_{drug} = \frac{E_{\max} \cdot C^{\gamma}}{EC_{50}{}^{\gamma} + C^{\gamma}} \tag{5}$$

$$k_{drug} = Slope \cdot C^{\gamma} \tag{6}$$

where E_{max} is the maximum achievable antibiotic-induced killing rate constant; EC_{50} is the antibiotic concentration that results in 50% of E_{max}; C is the drug concentration; and $Slope$ is the coefficient in a linear/power function.

Inh_{AR} represents the fractional decrease of k_{drug} and was restricted to be between 0 and 1. It is a function of the accumulated adaptive resistance AR_{ON} (Eq. 7):

$$Inh_{AR} = (1 - f(AR_{ON}))^{\beta} \tag{7}$$

where β was set to either 1 and $f(AR_{ON})$ restricted between 0 and 1, or to −1 and $f(AR_{ON})$ restricted to be negative. AR_{ON} is one of the two compartments that regulate resistance (Eqs. 8–10), as previously applied to colistin [9]:

$$\frac{dAR_{ON}}{dt} = k_{on} \cdot AR_{OFF} \quad (8)$$

$$\frac{dAR_{OFF}}{dt} = -k_{on} \cdot AR_{OFF} \quad (9)$$

$$k_{on} = f(C) \quad (10)$$

where AR_{OFF} and AR_{ON} are a pair of hypothetical adaptive resistance compartments of which the sum of the amount is always 1. Bacteria were assumed to be susceptible initially (AR_{OFF} was 1 and AR_{ON} was 0) and to gradually acquire resistance upon drug exposure (AR_{OFF} decreased towards 0 and AR_{ON} increased towards 1) with a rate governed by the antibiotic concentration-dependent constant k_{on}. A reversal transfer was not supported by the data. Tested functions for $f(AR_{ON})$ and $f(C)$ were (sigmoid) E_{max} and linear/power functions as described above (Eqs. 5 and 6) for k_{drug}.

A pre-existing resistant subpopulation model, as applied to meropenem [9], was also tested for both drugs. Two distinct subpopulations were assumed to exist in the starting inocula and the ratio of the two populations at this time point was estimated. The more resistant subpopulation had lower k_{drug} and potentially lower k_{growth} due to a fitness cost.

2.4.3. Combined drug modelling

A basic additive interaction model (Eq. 11) was used in the selection of combination time–kill experiments of interest:

$$k_{drug,COMB} = k_{drug,MIN} \cdot Inh_{AR,MIN} + k_{drug,PMB} \cdot Inh_{AR,PMB} \quad (11)$$

where $k_{drug,COMB}$ is the combined drug effect; $k_{drug,MIN}$ and $k_{drug,PMB}$ are the k_{drug} of MIN and PMB (Eqs. 5 and 6), respectively; and $Inh_{AR,MIN}$ and $Inh_{AR,PMB}$ are the Inh_{AR} of MIN and PMB (Eq. 7), respectively. After drug combination data had been generated, a general pharmacodynamic interaction (GPDI) function [18] was tested on various parameters such as k_{drug} (Eq. 12) and incorporated in Eq. 11 to evaluate the PMB and MIN interaction as victim and perpetrator drug:

$$k_{drug,vict,COMB} = k_{drug,vict,MONO} \cdot (1 + f(C_{perp})) \quad (12)$$

where $k_{drug,vict,MONO}$ and $k_{drug,vict,COMB}$ represent the k_{drug} of the victim drug before and after co-administration of the perpetrator drug whose impact is a function of the drug concentration $f(C_{perp})$. The tested functions were as described above (Eqs. 5 and 6). k_{drug} in Eq. 12 can be replaced by other drug-related parameters, e.g. k_{on}. When the two drugs are combined, the victim parameter is either stimulated [if $f(C_{perp}) > 0$], inhibited [if $-1 < f(C_{perp}) < 0$] or unaffected [if $f(C_{perp}) = 0$]. An empirical interaction model used by Mohamed et al. [9] (Eq. 8 in their article) was also tested.

2.4.4. Data analysis and model evaluation

In silico PKPD modelling was conducted using NONMEM® 7.4.2 with the Laplacian method. Model fit was mainly assessed by the objective function value (OFV) ($P < 0.001$, dOFV = 10.83, df. = 1). The transform-both-sides approach was applied to estimate the data using $\log_{10}$-transformed CFU/mL. The M3 method [19] was used to handle data below the LOD. The residual error was described by an additive error model, and the L2 data item [20] was applied to handle correlations among replicate samples plated from the same tube and time point. For nested models, the more complex model was selected only if the OFV decreased significantly. For non-nested models, the model with the lowest Akaike information criteria (AIC) value (AIC = OFV + 2p, where p is the number of estimated parameters) was selected. The interpretability of the model structure and the parameter values, together with the parameter precision, i.e. estimated relative standard errors (RSEs), were also considered. Perl-speaks-NONMEM (PsN) 4.7.15 (https://uupharmacometrics.github.io/PsN/) was used to facilitate modelling procedures. RStudio 3.5.1 (http://www.rstudio.com) was used for analysis visualisation.

Models were evaluated internally (with data used in the model development) and externally (with data not used in model development) by simulation-based VPCs (1000 sample size) [21]. For external evaluation, 22 time–kill curves from screening experiments, some of which were previously published [5], on the same strain were explored. The concentrations used were PMB at 1 mg/L and 2 mg/L and MIN at 4 mg/L and 16 mg/L, alone and in combination. The sampling timepoints were 0, 1, 3, 6 and 24 h. Consequently, neither the concentrations nor the timepoints were exactly the same as those used for model building.

2.5. Clinical drug effect predictions

The PK model by Sandri et al. [12] was chosen for PMB since it characterises two-compartment kinetics and has been commonly applied. The PK parameters from the population with creatinine clearance ≥75 mL/min by Welling et al. [11] was chosen for MIN since it is the only model reporting two-compartment parameters. The adopted PK model parameters are listed in Supplementary Table S1. A reported median PMB unbound drug fraction (f_u) of 42% [12] was used. The MIN f_u has been reported to be atypically concentration-dependent, i.e. decreasing f_u with increasing total concentration [22,23], like other members of the tetracycline family [24]. A log-linear model was fitted to the f_u data reported using HEPES buffer (pH controlled at 7.4, inert from divalent metal ions) [22]. The model (Eq. 13, Supplementary Fig. S1) indicated reduced f_u from ~60% to 12% when the total concentration (Ct) increased from 0.1 mg/L to 50 mg/L.

$$\ln(fu, \%) = 5.27 - 0.254 \cdot \ln(C_t, ug/L) \quad (13)$$

Considering that *K. pneumoniae* strain ARU613 has high MICs for both drugs, we chose to predict the combined drug effect based on the highest recommended doses, i.e. a loading dose (LD) of 2.5 mg/kg and a maintenance dose (MD) of 1.5 mg/kg every 12 h (q12h) for PMB [25] and a LD of 400 mg and a MD of 200 mg q12h for MIN [26]. All doses were infused intravenously over 1 h in the simulations. Additional simulated scenarios for comparison included standard doses of a LD of 2 mg/kg and a MD of 1.25 mg/kg q12h for PMB and a LD of 200 mg and a MD of 100 mg q12h for MIN; and a higher than typically used MIN dosage of 800 mg LD tapered by 100 mg per q12h dose until 400 mg [27]. Effects of monodrug and prolonged (4 h) infusion were also explored. In all scenarios, the starting inoculum was set to 6.8 $\log_{10}$ CFU/mL and 1000 patients per dosage were simulated. Interpatient variability in the PK profiles were considered. Simulations were done in mrgsolve (https://mrgsolve.github.io/).

3. Results

3.1. Time–kill experiments

In total, 88 time–kill curves were performed resulting in 1277 data points (Fig. 2a). A total of 41 data points were below the LOD, including 24 from MIN monodrug studies (5.2% of 460 observations), 16 from PMB monodrug studies (7.3% of 220 observations) and 1 from combination studies (0.2% of 597 observations).

Antibiotic effects clearly increased with increased drug concentrations (Fig. 2a). At concentrations of ≤0.5 × MIC, monodrug effects were marginal. At ~1 × MIC, bacterial density decreased

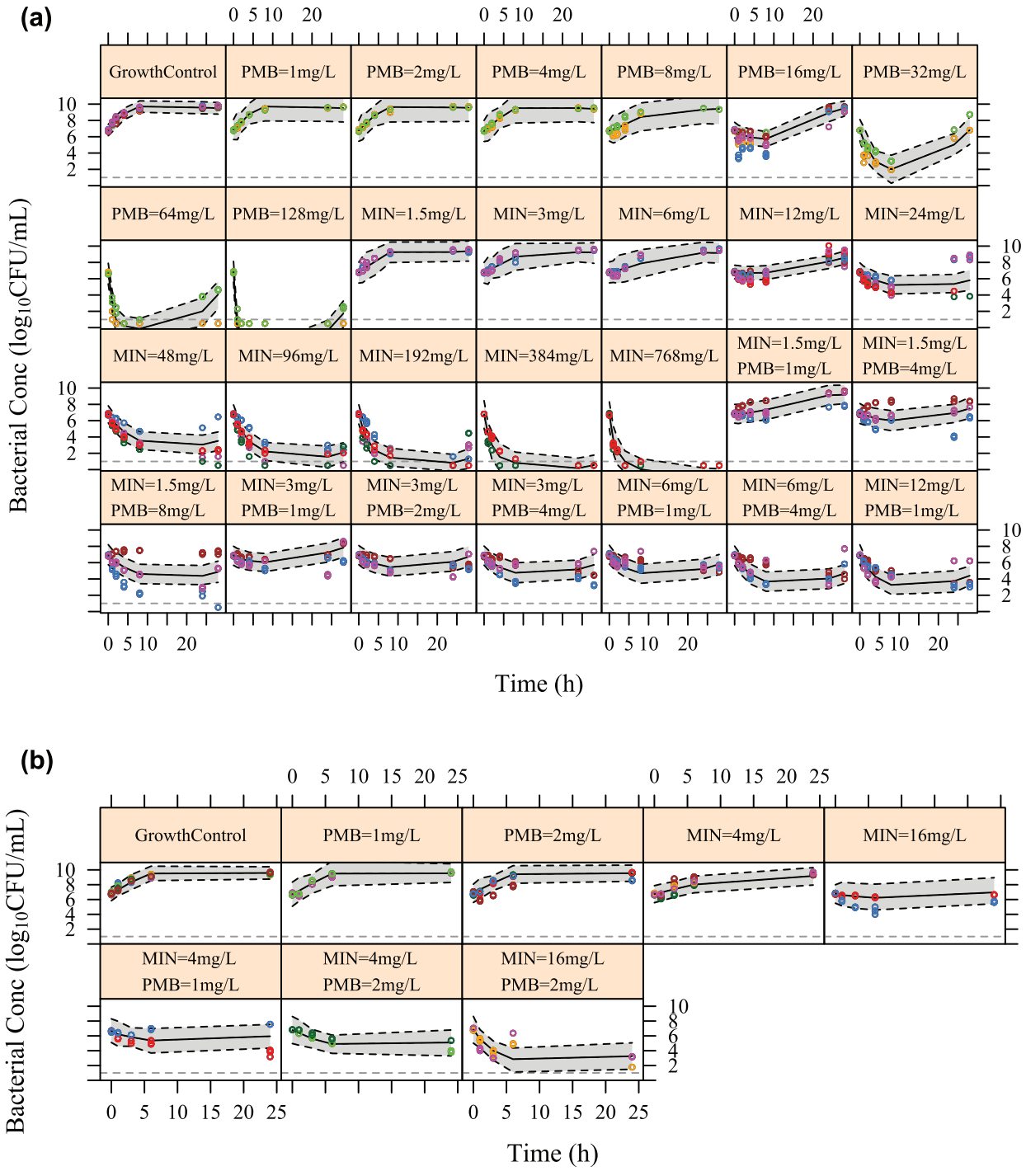

Fig. 2. Visual predictive checks for the final pharmacokinetic/pharmacodynamic model by (a) internal evaluation and (b) external evaluation. The observed bacterial concentrations are shown as open circles (coloured according to the respective experiment). The median (solid lines) and 95% confidence interval of the median (grey shade and black dashed lines) are defined from the data sets simulated from the model. Horizontal dashed lines indicate the limit of detection (LOD), with samples below the LOD presented below. Time–kill experiments of each dose level were performed on two to four occasions with typically more than one replicate CFU count per time point, defined from different dilutions. PMB, polymyxin B; MIN, minocycline.

in the first few hours, followed by re-growth. Concentrations of the component drugs in all combination studies were <1 × MIC. The improved killing effect compared with that of monodrug was noticeable. Eight of the nine tested concentration combinations showed synergism, defined as a ≥2 $\log_{10}$ CFU/mL (mean value of all replicates) decrease at 24 h with the combination compared with the effect of the best monodrug component at the same concentration. The only exception was the lowest concentrations tested (MIN 1.5 mg/L and PMB 1 mg/L), for which bacteriostasis was observed for 8 h before re-growth occurred.

3.2. Measured polymyxin B concentrations

The assayed start (0 h) concentrations were 0.14, 0.27, 0.75, 1.6, 3.3 and 8.0 mg/L for the nominal concentrations of 0.25, 0.5, 1, 2, 4 and 8 mg/L, respectively. This indicated a trend of an increasing extent of drug loss with decreasing nominal concentrations during preparation, i.e. from no loss at 8 mg/L up to 44% loss at 0.25 mg/L. The calculated corresponding k_d values were 0.175, 0.169, 0.120, 0.083, 0.023 and 0.022 h^{-1}, corresponding to half-lives of 4.0, 4.1, 5.8, 8.4, 30 and 32 h during the 0–4 h experimental period.

Table 2
Parameter estimates and precision of developed pharmacokinetic/pharmacodynamic model.

Parameter	Description	Estimated parameter (RSE)[a]	
Bacteria-related parameters			
k_{growth} (h^{-1})	Rate constant of bacterial growth	1.37 (13%)	
k_{death} (h^{-1})	Rate constant of natural bacterial death	0.179 (FIX) [b]	
B_{max} (CFU/mL)	Maximum bacterial concentration in system	10^9.53 (1%)	
T_{lag} (h)	Lag time for bacteria to transfer from S to R	0.304 (26%)	
Single drug-specific parameters		MIN	PMB
$Slope_1$ (L/mg/h)	Slope for power function of k_{drug}	0.339 (27%)	0.0690 (31%)
γ_1 (–)	Exponent for power function of k_{drug}	0.546 (10%)	1.20 (6%)
$Slope_2$ (L/mg/h)	Slope for linear function of k_{on}	0.000179 (33%)	0.00402 (16%)
$Slope_3$ (–)	Slope for linear function for AR	–10.2 (43%) [c]	1 (FIX)
Interaction parameters (PMB affecting MIN)			
E_{max} (–)	E_{max} for interaction function of $k_{drug,MIN,COMB}$	2.45 (28%)	
EC_{50} (mg/L)	EC_{50} for interaction function of $k_{drug,MIN,COMB}$	0.285 (71%) [c]	
$Slope_4$ (–)	Slope for interaction function of $k_{on,MIN,COMB}$	8.32 (27%)	
γ_4 (–)	Exponent for interaction function of $k_{on,MIN,COMB}$	0.479 (43%) [c]	
Residual error (SD, log_{10} CFU/mL)		0.907 (14%)	
Replicate residual error (SD, log_{10} CFU/mL)		0.164 (13%)	

S, susceptible compartment; R, resting compartment; MIN, minocycline; PMB, polymyxin B.
[a] RSE, relative standard error determined in NONMEM by $R^{-1}SR^{-1}$ (default) matrix.
[b] k_{death} was fixed to the value estimated in a previous study by Nielsen et al. [16].
[c] For parameters with reported RSE > 40%, their 95% confidence intervals were also computed by log-likelihood profiling. $Slope_3$: –6.36 to –18.3; EC_{50}: 0.0996–0.551; γ_4: 0.207–0.805.

3.3. In silico pharmacokinetic/pharmacodynamic model building

Fig. 1 shows the final PKPD model structure (NONMEM code is available upon request). Parameter estimates are listed in Table 2. Including a lag time for the bacteria transfer from S to R state significantly improved the model fit (dOFV = 65, estimate 0.3 h). k_{drug} was best described as a power function. A (sigmoid) E_{max} function was not supported by the data for either drug despite the fact that the experimental concentrations were >10 times higher than expected clinically. Adaptive resistance models fitted the data somewhat better than pre-existing resistance subpopulation models with the same number of parameters (dOFV = 20 for PMB and 24 for MIN). Inh_{AR} decreased with an increase in AR_{ON} (Eqs. 15 and 16). k_{on} increased linearly with antibiotic concentrations in the final model.

$$Inh_{AR,PMB} = 1 - AR_{ON,PMB} \tag{15}$$

$$Inh_{AR,MIN} = (1 - (-10.2) \cdot AR_{ON,MIN})^{-1} \tag{16}$$

GPDI functions best described the combined drug effect. The function with PMB as perpetrator and MIN as victim both for k_{drug} and k_{on} (Eqs. 17 and 18) described the drug interaction best. The PMB impact on MIN k_{on} (Eq. 18, dOFV = 135) was only significant after PMB impact on MIN k_{drug} (Eq. 17, dOFV = 133) was adopted into the model. MIN effect on PMB was insignificant in the final model.

$$k_{drug,MIN,COMB} = k_{drug,MIN} \cdot \left(1 + \frac{2.45 \cdot C_{PMB}}{0.285 + C_{PMB}}\right) \tag{17}$$

$$k_{on,MIN,COMB} = k_{on,MIN} \cdot \left(1 + 8.32 \cdot {C_{PMB}}^{0.479}\right) \tag{18}$$

According to Eqs. 17 and 18, the killing rate constant of MIN ($k_{drug,MIN}$) was predicted to increase 2.2-fold already at a relatively low PMB concentration (0.285 mg/L). The predicted MIN-induced resistance onset rate constant ($k_{on,MIN}$) increased 5.6-fold for the same PMB concentration. Both internal and external VPCs (Fig. 2) showed overall an adequate model fit, i.e. the typical trend of the observed data was similar to the medians in the data sets simulated from the model.

3.4. Clinical drug effect prediction

Both PMB and MIN as monodrugs showed marginal drug effects at an unbound concentration of ~2 mg/L (Fig. 3a). In comparison, a bacterial reduction upon combining these concentrations was evident (Fig. 3b). At PMB LD 2.5 mg/kg + MD 1.5 mg/kg and MIN LD 400 mg + MD 200 mg, the median trend stayed below the starting inoculum (bacteriostatic) for >20 h. The 4-h infusions had negligibly different CFU/mL profiles. The combined effects depended more on changes in MIN dose than on changes in PMB dose.

4. Discussion

In this study, a PKPD modelling strategy was applied to quantify the interaction between PMB and MIN against MDR-Kp from in vitro experimental data and to predict the clinical potential of the combination. The final PKPD model was the best based on an extensive structural model exploration with the mechanistic plausibility being considered. Mechanistically, the presented gradual decrease in antibiotic potency/efficacy, as characterised by an adaptive resistance model, may reflect a potential combined effect of exposure-induced resistance gene mutation/expression, selection of subpopulations, and loss of free antibiotics ready to exert an effect after binding to the dead cell debris. The identified one-way interaction model is in line with the common understanding that PMB disrupts cell membrane integrity leading to an increased intracellular MIN concentration and enhanced MIN bactericidal activity [28]. According to our model, PMB also accelerated resistance development against MIN. This may be because higher intracellular MIN exposure induces more resistance directly, or that the bacteria increase their tolerance to a higher degree when they are more severely affected. Despite the likely complex mechanisms of resistance and interaction in reality, a parsimonious (simple) model, with as few parameters as possible, that could adequately and reasonably characterise the data, was our aim.

The clinical effects predicted here assumed a central PK compartment site of infection, e.g. bloodstream infection, and a high bacterial concentration at the start of treatment similar to the starting inocula (6.8 log_{10} CFU/mL) in the time–kill experiments. To further illustrate the potential contribution of the immune sys-

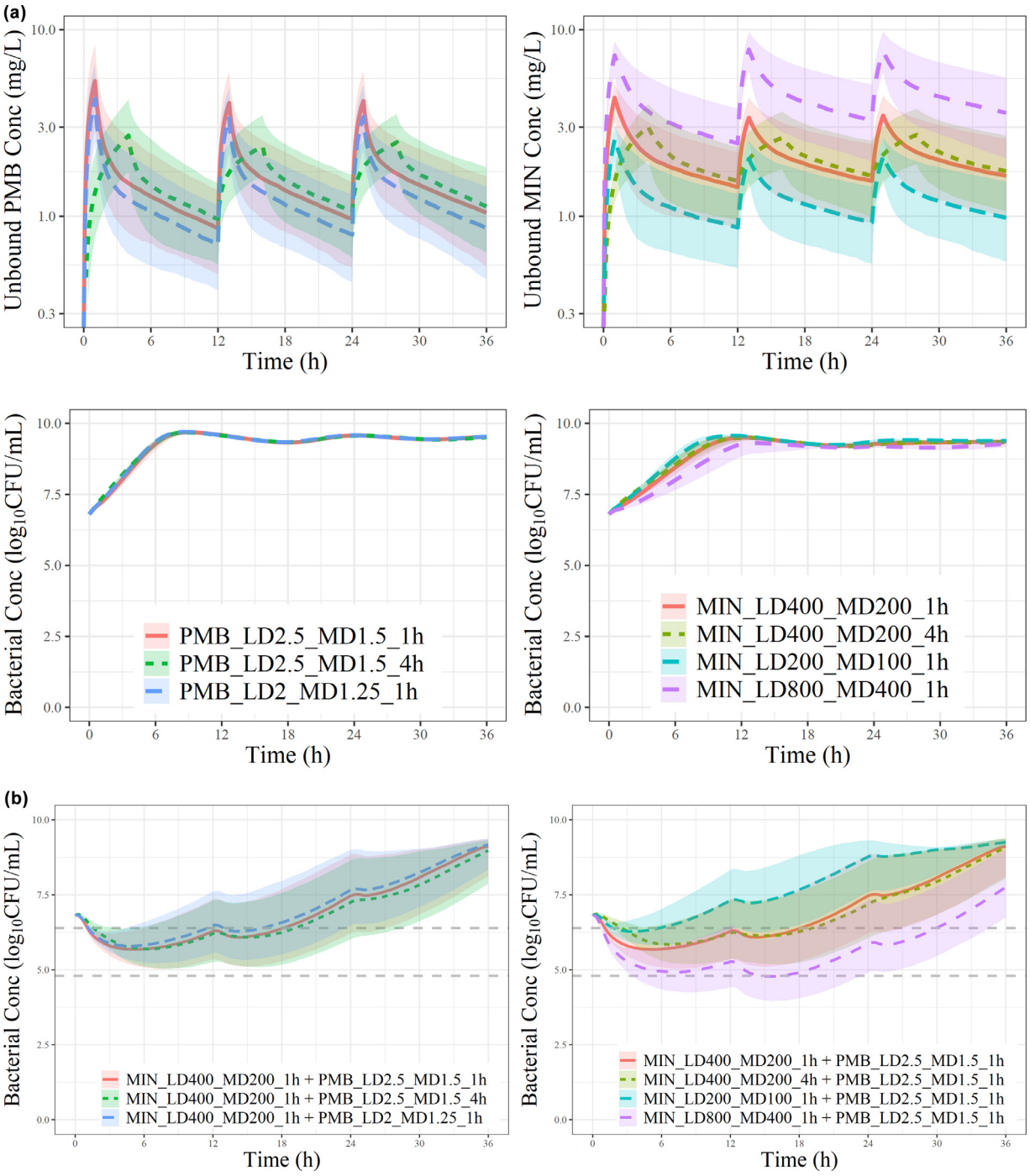

Fig. 3. Predicted antibiotic and bacterial concentration profiles over time when *Klebsiella pneumoniae* strain ARU613 is exposed to polymyxin B (PMB) and minocycline (MIN) (a) monodrug or (b) in combination over 36 h. Different colours in each panel represent the 50th (lines) and the 10th–90th percentile (shaded areas) profiles, i.e. prediction intervals, of 1000 simulated patients under different dosing scenarios. LD, loading dose; MD, maintenance dose; 1h, 1-h infusion; 4h, 4-h infusion. Numbers are the given doses (in mg/kg for PMB and mg for MIN). All doses are given every 12 h (q12h). For example, PMB_LD2.5_MD1.5_1h indicates that PMB is administrated by a loading dose of 2.5 mg/kg and a maintenance dose of 1.5 mg/kg q12h started from 12 h after the loading dose, all in a 1-h infusion. One exception is that MIN_LD800_MD400_1h indicates an 800 mg loading dose tapered by 100 mg per administration until 400 mg q12h, i.e. 800, 700, 600, 500 mg at 0, 12, 24, 36 h, respectively, all in a 1-h infusion in our simulation. Horizontal dashed lines in (b) indicate references for 2-$\log_{10}$ killing (i.e. 4.8 $\log_{10}$ CFU/mL) and burden for half saturated granulocyte-mediated killing (i.e. 6.4 $\log_{10}$ CFU/mL).

tem to the predicted CFU reduction, two reference lines are shown in Fig. 3b. The bacterial growth was reduced after treatment initiation in all simulated combination scenarios. The median nadir counts were predicted to be below 6.4 $\log_{10}$ CFU/mL, a threshold suggested to correspond to when granulocyte-mediated killing is half saturated [29]. When the MIN dosage was increased to a LD of 800 mg followed by tapering to a MD, a 2 $\log_{10}$ CFU/mL decrease from inoculum was reached, which would allow optimal contribution of granulocytes to bacterial clearance [29].

PMB + MIN has potential to broaden the clinical antimicrobial armament against MDR-Kp infections, especially when facing isolates with decreased susceptibility that would exclude monother-

apy by either drug. This combination has been reported to have been clinically used against *Acinetobacter* spp. [30] but to our knowledge not against *K. pneumoniae*. Earlier in vitro studies on polymyxins (two with colistin) + MIN against *K. pneumoniae* [31–33] have all suggested a positive combined effect, although the tested strains were susceptible to at least one of the drugs. That polymyxin-induced nephrotoxicity and neurotoxicity could be ameliorated by concomitant MIN [34,35] further supports the use of this combination from a safety perspective. Nevertheless, the predicted clinical antibacterial effects were moderate, but similar to what could be expected for a therapy against a strain with an MIC close to the clinical susceptibility breakpoint. It should be noted that (i) *K. pneumoniae* strain ARU613 is not susceptible to standard treatment and there would be a limited number of other treatment options, (ii) the combination displayed a much better effect than either drug alone, (iii) the combination is expected to achieve a better effect on strains with lower MICs, and (iv) the immune system is expected to assist in reducing the bacterial burden [29]. The highest simulated MIN dose in this study was reported to be safe and well tolerated in patients seeking neuroprotection [27], and it could consequently also be worth evaluating this dose in infected patients.

The translational approach applied here included the following steps:

1. in vitro time–kill studies and PKPD model building of each component drug alone;
2. design of combination studies aiming at concentrations being informative on the interaction;
3. conducting combination time–kill studies and exploring interaction functions in the PKPD model; and
4. predicting clinically achievable drug effect by linking the PKPD model to reported clinical PK profiles.

The direct translation from in vitro to clinical effect should, however, be interpreted with caution. Yet we have previously demonstrated that antibacterial effects of meropenem and colistin can translate well from in vitro to in vivo using a model-based strategy [36,37] and, based on these models, colistin and meropenem in combination have been predicted in patients [9]. We have also demonstrated the feasibility of models built on a similar data set to predict dynamic in vitro conditions [7], which implies that resource-demanding dynamic systems could be saved for verification, as a PKPD model based on static experiments can provide the same information as dynamic experiments. The strategy applied here illustrates a way to evaluate a combination identified in screening experiments by expanding the PD knowledge of the combination in in vitro static time–kill curves and by quantifying the interaction in a developed PKPD model that can subsequently be applied to explore the clinical potential. In contrast to the antibiotic PKPD index methodology, which is limited to monodrugs and does not consider that the index can be species-dependent owing to the different half-lives [36], our strategy can in a rational way forecast the relative effect of various combined dosing regimens, also in the presence of concentration-dependent drug interactions, as identified here. In addition, an independent effect of a functioning immune system could be added to the model in future explorations of translation to humans [38].

We did not attempt to validate the presumed data-driven mechanisms of resistance development with additional experimental data, which is a limitation of this study. Population analysis profiling, repeated MIC determination, and genetic characterisation of resistant populations may have shed more light on the reasons for re-growth and potential resistance mechanisms. Another potential limitation of this study is that since only one inoculum (6.8 $\log_{10}$ CFU/mL) was tested experimentally, it was not possible to evaluate the inoculum effect or any potential drug-induced killing of the resting bacteria. Nevertheless, the model with the same structure has been found to extrapolate reasonably well also when the bacteria have been allowed to grow to high bacterial counts before the antibiotic is added [39].

5. Conclusions

A PKPD model including adaptive resistance and one-way (PMB to MIN) interaction was developed to characterise the combined effect of PMB and MIN against MDR-Kp. The model predictions supported this combination as being a potential treatment option in face of difficult-to-treat isolates such as the strain studied here. This approach has promise to translate in vitro identified effective antibiotic therapies to dosage regimens worthwhile for in vivo and/or clinical studies.

Acknowledgment

The authors would like to thank Dr Richard Svensson [Uppsala University Drug Optimization and Pharmaceutical Profiling Platform (UDOPP), Sweden] for measuring antibiotic concentrations.

Funding: This work was supported by the Joint Programming Initiative on Antimicrobial Resistance (JPIAMR), Swedish Research Council [grant nos. 2015-06825 and 2015-06826].

Competing interests: None declared.

Ethical approval: Not required.

Supplementary material

Supplementary material associated with this article can be found, in the online version, at doi:10.1016/j.ijantimicag.2020.105941.

References

[1] Bassetti M, Righi E, Carnelutti A, Graziano E, Russo A. Multidrug-resistant *Klebsiella pneumoniae*: challenges for treatment, prevention and infection control. Expert Rev Anti Infect Ther 2018;16:749–61. doi:10.1080/14787210.2018.1522249.

[2] Tängdén T, Giske CG. Global dissemination of extensively drug-resistant carbapenemase-producing Enterobacteriaceae: clinical perspectives on detection, treatment and infection control. J Intern Med 2015;277:501–12. doi:10.1111/joim.12342.

[3] Tzouvelekis LS, Markogiannakis A, Psichogiou M, Tassios PT, Daikos GL. Carbapenemases in *Klebsiella pneumoniae* and other Enterobacteriaceae: an evolving crisis of global dimensions. Clin Microbiol Rev 2012;25:682–707. doi:10.1128/CMR.05035-11.

[4] Bergen PJ, Bulman ZP, Saju S, Bulitta JB, Landersdorfer C, Forrest A, et al. Polymyxin combinations: pharmacokinetics and pharmacodynamics for rationale use. Pharmacotherapy 2015;35:34–42. doi:10.1002/phar.1537.

[5] Wistrand-Yuen P, Olsson A, Skarp K-P, Friberg LE, Nielsen EI, Lagerbäck P, et al. Evaluation of polymyxin B in combination with 13 other antibiotics against carbapenemaseproducing *Klebsiella pneumoniae* in time-lapse microscopy and time-kill experiments. Clin Microbiol Infect 2020. doi:10.1016/j.cmi.2020.03.007.

[6] European Medicines Agency (EMA). Committee for Medicinal Products for Human Use (CHMP). Guideline on the use of pharmacokinetics and pharmacodynamics in the development of antimicrobial medicinal products.. London, UK: EMA; 2016 https://www.ema.europa.eu/en/documents/scientific-guideline/guideline-use-pharmacokinetics-pharmacodynamics-development-antimicrobial-medicinal-products_en.pdf [accessed 20 September 2019].

[7] Nielsen EI, Cars O, Friberg LE. Predicting in vitro antibacterial efficacy across experimental designs with a semimechanistic pharmacokinetic–pharmacodynamic model. Antimicrob Agents Chemother 2011;55:1571–9. doi:10.1128/AAC.01286-10.

[8] Brill MJE, Kristoffersson AN, Zhao C, Nielsen EI, Friberg LE. Semi-mechanistic pharmacokinetic–pharmacodynamic modelling of antibiotic drug combinations. Clin Microbiol Infect 2018;24:697–706. doi:10.1016/j.cmi.2017.11.023.

[9] Mohamed AF, Kristoffersson AN, Karvanen M, Nielsen EI, Cars O, Friberg LE. Dynamic interaction of colistin and meropenem on a WT and a resistant strain of *Pseudomonas aeruginosa* as quantified in a PK/PD model. J Antimicrob Chemother 2016;71:1279–90. doi:10.1093/jac/dkv488.

[10] Karvanen M, Malmberg C, Lagerbäck P, Friberg LE, Cars O. Colistin is extensively lost during standard in vitro experimental conditions. Antimicrob Agents Chemother 2017:61 pii: e00857-17. doi:10.1128/AAC.00857-17.
[11] Welling PG, Shaw WR, Uman SJ, Tse FL, Craig WA. Pharmacokinetics of minocycline in renal failure. Antimicrob Agents Chemother 1975;8:532–7. doi:10.1128/AAC.8.5.532.
[12] Sandri AM, Landersdorfer CB, Jacob J, Boniatti MM, Dalarosa MG, Falci DR, et al. Population pharmacokinetics of intravenous polymyxin B in critically ill patients: implications for selection of dosage regimens. Clin Infect Dis 2013;57:524–31. doi:10.1093/cid/cit334.
[13] European Committee on Antimicrobial Susceptibility Testing (EUCAST). Breakpoint tables for interpretation of MICs and zone diameters. Version 9.0, 2019.. EUCAST; 2019 http://www.eucast.org/clinical_breakpoints/ [accessed 19 March 2020].
[14] Clinical and Laboratory Standards Institute (CLSI). Performance standards for antimicrobial susceptibility testing. 30th ed. Wayne, PA: CLSI; 2020. CLSI supplement M100.
[15] Jansson B, Karvanen M, Cars O, Plachouras D, Friberg LE. Quantitative analysis of colistin A and colistin B in plasma and culture medium using a simple precipitation step followed by LC/MS/MS. J Pharm Biomed Anal 2009;49:760–7. doi:10.1016/j.jpba.2008.12.016.
[16] Nielsen EI, Viberg A, Löwdin E, Cars O, Karlsson MO, Sandström M. Semimechanistic pharmacokinetic/pharmacodynamic model for assessment of activity of antibacterial agents from time–kill curve experiments. Antimicrob Agents Chemother 2007;51:128–36. doi:10.1128/AAC.00604-06.
[17] Brauner A, Fridman O, Gefen O, Balaban NQ. Distinguishing between resistance, tolerance and persistence to antibiotic treatment. Nat Rev Microbiol 2016;14:320–30. doi:10.1038/nrmicro.2016.34.
[18] Wicha SG, Chen C, Clewe O, Simonsson USH. A general pharmacodynamic interaction model identifies perpetrators and victims in drug interactions. Nat Commun 2017;8:2129. doi:10.1038/s41467-017-01929-y.
[19] Ahn JE, Karlsson MO, Dunne A, Ludden TM. Likelihood based approaches to handling data below the quantification limit using NONMEM VI. J Pharmacokinet Pharmacodyn 2008;35:401–21. doi:10.1007/s10928-008-9094-4.
[20] Karlsson MO, Beal SL, Sheiner LB. Three new residual error models for population PK/PD analyses. J Pharmacokinet Biopharm 1995;23:651–72. doi:10.1007/BF02353466.
[21] Karlsson MO, Holford N. A tutorial on visual predictive checks. In: Abstracts of the Annual Meeting of the Population Approach Group in Europe; 18–20 June 2008; Marseille, France. PAGE; 2008.
[22] Dorn C, Kratzer A, Liebchen U, Schleibinger M, Murschhauser A, Schlossmann J, et al. Impact of experimental variables on the protein binding of tigecycline in human plasma as determined by ultrafiltration. J Pharm Sci 2018;107:739–44. doi:10.1016/j.xphs.2017.09.006.
[23] Zhou J, Tran BT, Tam VH. The complexity of minocycline serum protein binding. J Antimicrob Chemother 2017;72:1632–4. doi:10.1093/jac/dkx039.
[24] Nation RL, Theuretzbacher U. Tsuji BT; International Society of Anti-Infective Pharmacology (ISAP). Concentration-dependent plasma protein binding: expect the unexpected. Eur J Pharm Sci 2018;122:341–6. doi:10.1016/j.ejps.2018.07.004.
[25] Tsuji BT, Pogue JM, Zavascki AP, Paul M, Daikos GL, Forrest A, et al. International consensus guidelines for the optimal use of the polymyxins: endorsed by the American College of Clinical Pharmacy (ACCP), European Society of Clinical Microbiology and Infectious Diseases (ESCMID), Infectious Diseases Society of America (IDSA), International Society for Anti-infective Pharmacology (ISAP), Society of Critical Care Medicine (SCCM), and Society of Infectious Diseases Pharmacists (SIDP). Pharmacotherapy 2019;39:10–39. doi:10.1002/phar.2209.
[26] Melinta Therapeutics. MINOCIN® (minocycline for injection). Melinta Therapeutics; 2019 http://www.minociniv.com/pdfs/minocin-us-prescribing-information.pdf [accessed 20 September 2019].
[27] Casha S, Zygun D, McGowan MD, Bains I, Yong VW, John Hurlbert R. Results of a phase II placebo-controlled randomized trial of minocycline in acute spinal cord injury. Brain 2012;135:1224–36. doi:10.1093/brain/aws072.
[28] Bowers DR, Cao H, Zhou J, Ledesma KR, Sun D, Lomovskaya O, et al. Assessment of minocycline and polymyxin B combination against *Acinetobacter baumannii*. Antimicrob Agents Chemother 2015;59:2720–5. doi:10.1128/AAC.04110-14.
[29] Drusano GL, Liu W, Fikes S, Cirz R, Robbins N, Kurhanewicz S, et al. Interaction of drug- and granulocyte-mediated killing of *Pseudomonas aeruginosa* in a murine pneumonia model. J Infect Dis 2014;210:1319–24. doi:10.1093/infdis/jiu237.
[30] Lashinsky JN, Henig O, Pogue JM, Kaye KS. Minocycline for the treatment of multidrug and extensively drug-resistant *A. baumannii*: a review. Infect Dis Ther 2017;6:199–211. doi:10.1007/s40121-017-0153-2.
[31] Huang D, Yu B, Diep JK, Sharma R, Dudley M, Monteiro J, et al. In vitro assessment of combined polymyxin B and minocycline therapy against *Klebsiella pneumoniae* carbapenemase (KPC)-producing *K. pneumoniae*. Antimicrob Agents Chemother 2017;61 pii: e00073-17. doi:10.1128/AAC.00073-17.
[32] Brennan-Krohn T, Truelson KA, Smith KP, Kirby JE. Screening for synergistic activity of antimicrobial combinations against carbapenem-resistant Enterobacteriaceae using inkjet printer-based technology. J Antimicrob Chemother 2017;72:2775–81. doi:10.1093/jac/dkx241.
[33] MacNair CR, Stokes JM, Carfrae LA, Fiebig-Comyn AA, Coombes BK, Mulvey MR, et al. Overcoming *mcr-1* mediated colistin resistance with colistin in combination with other antibiotics. Nat Commun 2018;9:458. doi:10.1038/s41467-018-02875-z.
[34] Lodise TP, Fan W, Griffith DC, Dudley MN, Sulham KA. A retrospective cohort analysis shows that coadministration of minocycline with colistin in critically ill patients is associated with reduced frequency of acute renal failure. Antimicrob Agents Chemother 2018;62 pii: e01165-17. doi:10.1128/AAC.01165-17.
[35] Dai C, Ciccotosto GD, Cappai R, Wang Y, Tang S, Xiao X, et al. Minocycline attenuates colistin-induced neurotoxicity via suppression of apoptosis, mitochondrial dysfunction and oxidative stress. J Antimicrob Chemother 2017;72:1635–45. doi:10.1093/jac/dkx037.
[36] Kristoffersson AN, David-Pierson P, Parrott NJ, Kuhlmann O, Lave T, Friberg LE, et al. Simulation-based evaluation of PK/PD indices for meropenem across patient groups and experimental designs. Pharm Res 2016;33:1115–25. doi:10.1007/s11095-016-1856-x.
[37] Khan DD, Friberg LE, Nielsen EI. A pharmacokinetic–pharmacodynamic (PKPD) model based on in vitro time–kill data predicts the in vivo PK/PD index of colistin. J Antimicrob Chemother 2016;71:1881–4. doi:10.1093/jac/dkw057.
[38] Sadiq MW, Nielsen EI, Khachman D, Conil JM, Georges B, Houin G, et al. A whole-body physiologically based pharmacokinetic (WB-PBPK) model of ciprofloxacin: a step towards predicting bacterial killing at sites of infection. J Pharmacokinet Pharmacodyn 2017;44:69–79. doi:10.1007/s10928-016-9486-9.
[39] Nielsen EI, Khan DD, Cao S, Lustig U, Hughes D, Andersson DI, et al. Can a pharmacokinetic/pharmacodynamic (PKPD) model be predictive across bacterial densities and strains? External evaluation of a PKPD model describing longitudinal in vitro data. J Antimicrob Chemother 2017;72:3108–16. doi:10.1093/jac/dkx269.